

Importance of Laplacian of low-level warming for the response of precipitation to climate change over tropical oceans

Margaret L. Duffy, Paul A. O’Gorman, Larissa E. Back
Supplementary material

Supplementary text: Further discussion of the role of weakening of the tropical circulation

Previous studies have found that the tropical divergent circulation weakens under projected climate change (e.g., Vecchi and Soden (2007)), and it is clear from the DSE budget (or moisture budget) that the resulting changes in vertical velocities should lead to a dynamic contribution to changes in precipitation. Part of the weakening of the circulation is related to the pattern of SST change (He and Soden, 2015) and this affects precipitation in our framework through the effect of both SST_{rel} and $\nabla^2 SST$ on the shallow and deep modes. Indeed, a partial compensation between wet get wetter and the contribution from changes in SC is evident in Fig 2. However, part of the weakening of the circulation relates to the spatial-mean component of the SST change and to increases in CO_2 (Ma et al., 2012; He and Soden, 2015; Merlis, 2015) and these are not captured by our relations of the deep and shallow mode amplitudes to SST_{rel} and $\nabla^2 SST$, although they may be partly included in the two-mode model when SC(GCM) is used.

The AMIP_4K simulations help to quantify the importance of circulation weakening due to spatial-mean warming since these simulations have a spatially uniform increase in SST (Fig. S1). Circulation changes related to spatial-mean warming in AMIP_4K may contribute to discrepancies between the GCM changes in precipitation and those from the two-mode model (e.g., in the central Pacific in Fig. S1a,b) and to the small changes in SC that occur despite a spatially uniform SST increase (Fig. S1f). Nonetheless, the AMIP_4K precipitation response resembles the wet-get-wetter contribution and the difference between them does not resemble a weakening of the climatological precipitation pattern. Thus the contribution of a weakening circulation from spatial-mean warming does not seem to be a dominant contributor to the precipitation response. The weakening of the circulation is often measured by changes in ω at 500hPa, and we have confirmed that the two-mode model with unapproximated o_s and o_d captures a weakening of ω at 500hPa at a rate of $3.6\% K^{-1}$ as measured based on regression over ascent regions of the tropical oceans under AMIP_4K, though there is a large spread in the response that is not captured by the regression. Part of this weakening of ω at 500hPa comes from changes in the vertical structures of the modes ($0.9\% K^{-1}$) but most of it comes from changes in o_s and o_d ($2.7\% K^{-1}$). The contribution to ΔP from changes in o_s and o_d is a smaller weakening of $1.9\% K^{-1}$ as measured by regression for AMIP_4K, but this contribution has both positive and negative values and again there is a large spread in the response that is not captured by the regression. This large spread explains why the difference between the total AMIP_4K precipitation response and the wet-get-wetter contribution does not resemble a weakening of the climatological precipitation (Fig. S1).

For RCP8.5 which includes both spatial-mean warming and changes in SST gradients, Chadwick et al. (2013) found that a dynamical weakening offset much of the wet-get-wetter (thermodynamic) component of the precipitation response in the tropics. They defined the thermodynamic component as the increase in precipitation at fixed convective mass flux, and this thermodynamic component scales with the low-level specific humidity at $7\% K^{-1}$. By contrast, we define wet get wetter as the contribution due to changes in M_{ses} and M_{sed} which gives a rate of increase of $5.6\% K^{-1}$ as measured by regression for AMIP_4K.¹ Thus, less of a dynamical weakening is needed in our formulation based on the DSE budget because of a smaller thermodynamic rate of increase as compared to the low-level specific humidity framework used by Chadwick et al. (2013).

¹Most of this contribution comes from increases in $-\frac{\partial s}{\partial p}$ ($5.1\% K^{-1}$) with smaller contributions from changes in the vertical structure functions ($0.9\% K^{-1}$) and from changes in radiation regression coefficients ($-0.4\% K^{-1}$). The $5.1\% K^{-1}$ from changes in $-\frac{\partial s}{\partial p}$ is different from the $3.5\% K^{-1}$ found in Muller and O’Gorman (2011) largely because Muller and O’Gorman (2011) normalize by global-mean surface warming whereas we normalize by surface warming over the tropical oceans.

References

- Chadwick, R., I. Boutle, and G. Martin, 2013: Spatial patterns of precipitation change in CMIP5: Why the rich do not get richer in the tropics. *J. Climate*, **26**, 3803–3822, doi:10.1175/JCLI-D-12-00543.1.
- He, J., and B. J. Soden, 2015: Anthropogenic weakening of the tropical circulation: The relative roles of direct CO₂ forcing and sea surface temperature change. *J. Climate*, **28**, 8728–8742, doi:10.1175/JCLI-D-15-0205.1.
- Ma, J., S.-P. Xie, and Y. Kosaka, 2012: Mechanisms for tropical tropospheric circulation change in response to global warming. *J. Climate*, **25**, 2979–2994, doi:10.1175/JCLI-D-11-00048.1.
- Merlis, T. M., 2015: Direct weakening of tropical circulations from masked CO₂ radiative forcing. *Proc. Natl. Acad. Sci.*, **112**, 13 167–13 171.
- Muller, C. J., and P. A. O’Gorman, 2011: An energetic perspective on the regional response of precipitation to climate change. *Nat. Climate Change*, **1**, 266–271, doi:10.1038/nclimate1169.
- Vecchi, G. A., and B. J. Soden, 2007: Global warming and the weakening of the tropical circulation. *J. Climate*, **20**, 4316–4340, doi:10.1175/jcli4258.1.

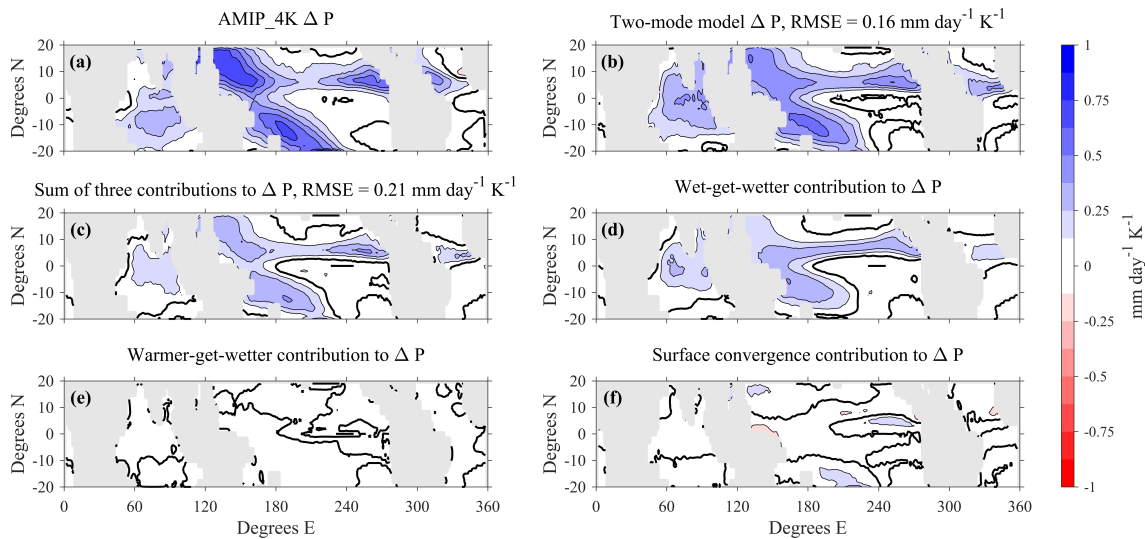


Figure S1: As in Fig. 2 except for AMIP_4K simulation. Contour interval: 0.125 mm day⁻¹ K⁻¹.

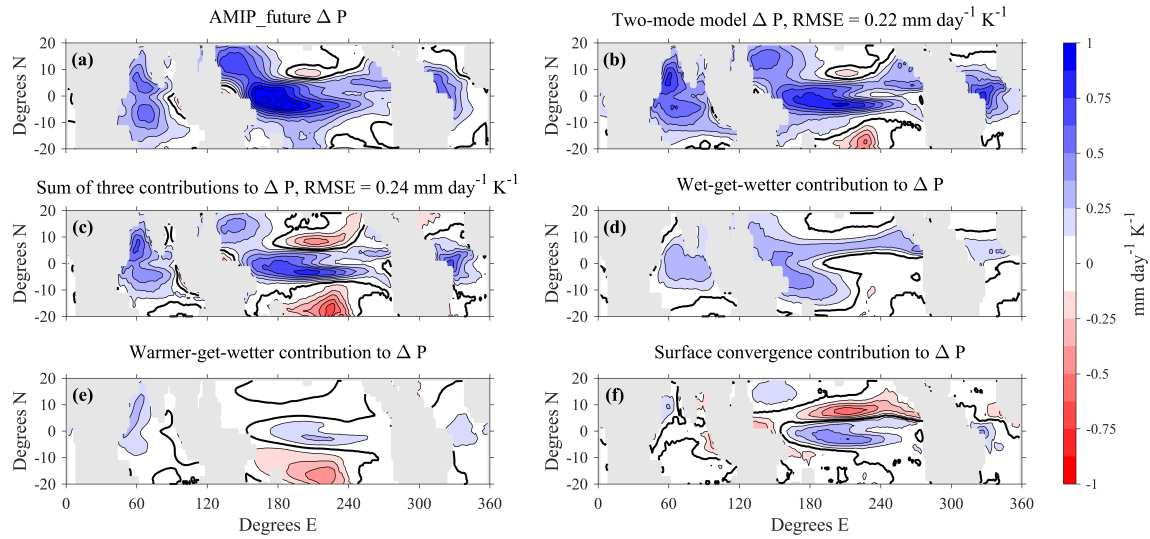


Figure S2: As in Fig. 2 except for AMIP_future simulation. Contour interval: $0.125 \text{ mm day}^{-1} \text{K}^{-1}$.

Table S1: List of GCMs used. Different subsets of GCMs are used in the two-mode model analysis in Section 3, in the MLM analysis in Sections 4 and 5, and in the AMIP analysis in Section 6, as indicated by the presence of an RMSE values. Values in the first column are the RMSE values for ΔP from the two-mode model for the RCP8.5 scenario (as compared to ΔP from the GCM). Values in the second column are RMSE values for $\Delta SC(\nabla^2 T_v)$ and $\Delta SC(\nabla^2 SST)$ for the RCP8.5 scenario, each as compared to $\Delta SC(\text{GCM})$. Values in the third column are RMSE values for ΔP from the two-mode model for AMIP_pattern

	Two-mode model	MLM	AMIP
	RMSE ΔP	RMSE $\Delta SC(\nabla^2 T_v)$, $\Delta SC(\nabla^2 SST)$	RMSE ΔP AMIP_pattern
	mm day ⁻¹	s ⁻¹	mm day ⁻¹ K ⁻¹
ACCESS1.0	1.46	1.04e-6, 2.06e-6	
ACCESS1.3	1.58	1.27e-6, 2.34e-6	
CanAM4			0.22
CanESM2	1.44		
CMCC-CESM	1.57		
CMCC-CM	1.57		
CMCC-CMS	1.41		
CNRM-CM5	0.72		0.22
CSIRO Mk3.6.0	1.73		
GFDL-CM3	1.34	1.07e-6, 1.89e-6	
GFDL-ESM2G	0.89	1.10e-6, 1.64e-6	
GFDL-ESM2M	1.16	1.10e-6, 1.44e-6	
HadGEM2-A			0.28
HadGEM2-ES	1.50	1.17e-6, 2.61e-6	
INM-CM4.0	0.83	8.18e-7, 1.69e-6	
IPSL-CM5A-LR			0.40
IPSL-CM5A-MR	1.32	1.01e-6, 1.74e-6	
IPSL-CM5B-LR			0.23
MIROC5	1.32		0.27
MIROC-ESM	1.07		
MPI-ESM-MR	1.19		
MRI-CGCM3	1.45	9.81e-7, 1.79e-6	0.35
MRI-ESM1	1.52	9.84e-7, 1.78e-6	
NorESM1-M	1.29	1.29e-6, 1.87e-6	

Table S2: Two-mode model coefficients for ERA-Interim and for the ensemble mean of the two CMIP5 simulations and the three AMIP simulations used throughout the paper. The ERA-Interim version of the two-mode model use NOAA optimal interpolation SST and QuikSCAT SC observations (see Section 2c of text). In the ERA-Interim version $\nabla^2 T_v$ and $\nabla^2 \text{SST}$ are spatially smoothed. First section: Radiation regression coefficients (Eq. 3). Second section: Two-mode model coefficients (Eq. 7). Third section: Deep-mode regression coefficients when $\text{SC}(\nabla^2 T_v)$ is used (Fig. 6d). Fourth section: Deep-mode regression coefficients when $\text{SC}(\nabla^2 \text{SST})$ is used (Fig.6e).

Constant	ERA-I	CMIP5 hist	CMIP5 RCP8.5	AMIP_control	AMIP_4K	AMIP_future
r_s (m)	-42.1	-44.9	-60.2	-37.8	-70.4	-76.0
r_d (m)	232.3	217.3	244.6	228.0	263.2	258.9
R_0 (W m^{-2})	-119.9	-115.7	-120.9	-116.4	-130.1	-131.0
M_{ses} (m)	505.7	476.3	535.2	482.1	524.5	532.3
M_{sed} (m)	819.9	792.7	966.5	779.1	1014.6	1055.2
a_s (Pa)	1.90e4	1.90e4	1.86e4	2.1e4	1.98e4	2.02e4
b_{SST} ($\text{Pa s}^{-1} \text{K}^{-1}$)	0.0670	0.0571	0.0543	0.0669	0.0695	0.0681
b_{SC} (Pa)	1.52e4	2.27e4	2.28e4	2.24e4	2.22e4	2.39e4
b_0 (Pa s^{-1})	-0.0584	-0.0383	-0.0348	-0.0485	-0.045	-0.0379
b_{SST} ($\text{Pa s}^{-1} \text{K}^{-1}$)	0.0783	0.0787	0.0755	0.0797	0.0808	0.0795
$b_{\text{SC}(\nabla^2 T_v)}$ (Pa)	1.00e4	1.23e4	1.13e4	1.25e4	1.16e4	0.91e4
b_0 (Pa s^{-1})	-0.0555	-0.0435	-0.0407	-0.0451	-0.0398	-0.0274
b_{SST} ($\text{Pa s}^{-1} \text{K}^{-1}$)	0.0739	0.0787	0.0734	0.075	0.0763	0.075
$b_{\text{SC}(\nabla^2 \text{SST})}$ (Pa)	3170.3	1747.9	2114.4	2901.5	2898.1	987.7
b_0 (Pa s^{-1})	-0.0424	-0.0262	-0.0240	-0.0284	-0.0245	-0.0123